Journal of Hazardous Materials 445 (2023) 130581

Contents lists available at ScienceDirect

Journal of Hazardous Materials

journal homepage: www.elsevier.com/locate/jhazmat

Research Paper

Contrasting Cd accumulation of *Arabidopsis halleri* populations: a role for (1→4)-β-galactan in pectin

Xinhui An [a], Jean-Chrisologue Totozafy [b], Alexis Peaucelle [b], Catherine Yvonne Jones [c], William G.T. Willats [c], Herman Höfte [b], Massimiliano Corso [a,b,*,1], Nathalie Verbruggen [a,**,1]

[a] *Laboratory of Plant Physiology and Molecular Genetics, Université Libre de Bruxelles, 1050 Brussels, Belgium*
[b] *Université Paris-Saclay, INRAE, AgroParisTech, Institut Jean-Pierre Bourgin (IJPB), 78000 Versailles, France*
[c] *School of Natural and Environmental Sciences, Newcastle University, Newcastle upon Tyne, UK*

HIGHLIGHTS

- PL22-H pectins contained a higher Cd concentration than I16-E pectins in root CWs.
- *GALS1* expression and (1→4)-β-galactan content were different between PL22-H and I16-E.
- *GALS1* mutants showed longer RGI sidechains in root CW and higher metal translocations.
- (1→4)-β-galactan indirectly impacts Cd flux probably by modifying the CW structure.
- Expression *BDX* and *LUH* seem to also impact metal accumulation, in particular Zn.

GRAPHICAL ABSTRACT

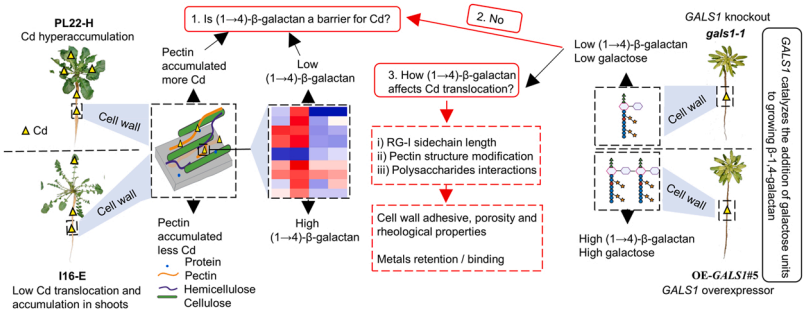

ARTICLE INFO

Editor: Wagner L. Araújo

Keywords:
Cell wall
Cd excluder
Hyperaccumulator
Polysaccharides
Structure modification

ABSTRACT

Cadmium (Cd) accumulation is highly variable among *Arabidopsis halleri* populations. To identify cell wall (CW) components that contribute to the contrasting Cd accumulation between PL22-H (Cd-hyperaccumulator) and I16-E (Cd-excluder), Cd absorption capacity of CW polysaccharides, CW mono- and poly- saccharides contents and CW glycan profiles were compared between these two populations. PL22-H pectin contained 3-fold higher Cd concentration than I16-E pectin in roots, and (1→4)-β-galactan pectic epitope showed the biggest difference between PL22-H and I16-E. CW-related differentially expressed genes (DEGs) between PL22-H and I16-E were identified and corresponding *A. thaliana* mutants were phenotyped for Cd tolerance and accumulation. A higher Cd translocation was observed in *GALACTAN SYNTHASE1 A. thaliana* knockout and overexpressor mutants, which both showed a lengthening of the RG-I sidechains after Cd treatment, contrary to the wild-type. Overall,

Abbreviations: Cd, Cadmium; PL22-H, PL22 Cd-hyperaccumulator; I16-E, I16 Cd-excluder; DEG, Differentially Expressed Genes; TM, Trace Metal; CW, Cell Wall; PE, Pectin; HC, Hemicellulose; HG, Homogalacturonan; RG-I, Rhamnogalacturonan-I; Ara, Arabinose; Gal, Galactose; GalA, Galacturonic acid; Rha, Rhamnose; WT, Wild-Type.

* Corresponding author at: Université Paris-Saclay, INRAE, AgroParisTech, Institut Jean-Pierre Bourgin (IJPB), 78000 Versailles, France.
** Corresponding author.
E-mail addresses: Xinhui.an@ulb.be (X. An), jean-chrisologue.totozafy@inrae.fr (J.-C. Totozafy), alexis.peaucelle@inrae.fr (A. Peaucelle), catherine.tetard-jones@ncl.ac.uk (C.Y. Jones), william.willats@newcastle.ac.uk (W.G.T. Willats), hermanus.hofte@inrae.fr (H. Höfte), massimiliano.corso@inrae.fr (M. Corso), nathalie.verbruggen@ulb.be (N. Verbruggen).
[1] Equal contribution

https://doi.org/10.1016/j.jhazmat.2022.130581
Received 23 July 2022; Received in revised form 2 November 2022; Accepted 7 December 2022
Available online 9 December 2022

our results support an indirect role for (1→4)-β-galactan in Cd translocation, possibly by a joint effect of regulating the length of RG-I sidechains, the pectin structure and interactions between polysaccharides in the CW. The characterization of other CW-related DEGs between I16-E and PL22-H selected allowed to identify a possible role in Zn translocation for *BIIDXI* and *LEUNIG-HOMOLOG* genes, which are both involved in pectin modification.

1. Introduction

Cadmium (Cd) is a major trace metal (TM) contaminant in our environment that poses a potential health risk to humans through food chains (Chaffei, 2003; Gouia et al., 2003; Grant et al., 2008; Hu et al., 2013; Åkesson et al., 2014; Genchi et al., 2020; Suhani et al., 2021). The World Health Organization (WHO) classified Cd as one of the *"top ten chemicals of major health concern"* based on scientific evidence and risk management (https://www.who.int/news-room/photo-story/photo-story-detail/10-chemicals-of-public-health-concern). In plants, Cd is a non-essential element, which is absorbed in roots via transporters for essential divalent cations such as calcium (Ca), iron (Fe), manganese (Mn), zinc (Zn) and copper (Cu) (Papoyan and Kochian, 2004; Pittman et al., 2004; Koren'kov et al., 2007; Verbruggen et al., 2009a; Chen et al., 2018). Therefore, Cd toxicity has been partially attributed to the perturbation of the homeostasis of essential elements (Siedlecka and BaszyńAski, 1993; Schutzendubel and Polle, 2002; Clemens, 2006). Moreover, Cd reduced seed germination, plant biomass, induced oxidative stress, altered plant photosynthesis, respiration and transpiration rate (El Rasafi et al., 2022; Loix et al., 2017). While most plants are susceptible to Cd toxicity, some metallophytes are hypertolerant to Cd. Most of these plants are Cd excluders, since they are able to limit Cd entry in the roots and/or Cd transfer from roots to the shoots. A rare category of metallophytes are Cd hyperaccumulators, which can accumulate Cd in the shoots above 100 ppm without toxicity symptoms (Baker, 1981; Baker et al., 2020). The hyperaccumulation phenomenon has been extensively studied, while molecular and biochemical mechanisms driving Cd-exclusion have been less investigated in plants, despite the potential application for limiting Cd accumulation in crops (Clemens et al., 2013; Clemens and Ma, 2016; Clemens, 2019).

Arabidopsis halleri constitutively hyperaccumulates Zn and some populations can also hyperaccumulate Cd. *A. halleri* is a model to study adaptation to extreme metallic environments and metal homeostasis (Verbruggen et al., 2009b, 2013; Krämer, 2010; Hanikenne and Nouet, 2011). This species is a clonal, self-incompatible, diploid and highly outcrossing perennial Brassicaceae showing much higher Cd tolerance than the genetically related *A. thaliana* and *A. lyrata* species (Meyer et al., 2015). *A. halleri* populations are mainly distributed into three European Genetic Units (GU), according to their geographical origin, namely the Hybrid Zone, South-Eastern and North-Western GUs (Pauwels et al., 2012). PL22-H originates from the "Hybrid Zone" GU (south of Poland) and behaves as a Cd hyperaccumulator, while I16-E grows in the South-East GU (north of Italy) and shows limited Cd accumulation in shoots (Meyer et al., 2015; Corso et al., 2018, 2021). Previous transcriptomic studies of PL22-H and I16-E identified the cell wall (CW) as a potential major player in *A. halleri* adaptation to metalliferous soils (Corso et al., 2018, 2021; Schvartzman et al., 2018), paving the way for further study the role played by the specific CW component in TM hyperaccumulation and exclusion.

The root is the first organ that comes into contact with TM-contaminated soils and regulates the entrance of TM. Cd accumulation in shoots indeed largely depends on root properties (Clemens, 2006; Guimarães et al., 2009). The CW of root cells serves as the first barrier to prevent Cd from entering into the cytoplasm. Primary CW consists of pectin (PE), hemicellulose (HC), cellulose polysaccharides and structural proteins, such as extensin and arabinogalactan proteins. These proteins are embedded in a complex network of polysaccharides (Rose, 2003). PE is a polysaccharide-based polymer, composed of galacturonic acid (GalA) and rhamnose (Rha) backbones, and sidechains made up of arabinose, fucose, galactose and xylose (Rose, 2003). HC is a heteropolymer that consists of diverse sugar carbohydrates, including mannose, galactose, glucose, xylose, arabinose and 4-O-methyl-D-glucuronic acid (Bajpai, 2018). PE and HC polymers contain negatively charged functional groups such as hydroxyl, thiol and carboxyl, which can bind divalent and trivalent metals. They play important roles in TMs immobilization (Wei et al., 2008; Yang et al., 2008; Krzesłowska, 2011; Loix et al., 2017). Previous studies showed that higher uronic acid or sugar content in PE and HC induced a greater Cd holding capacity in the CW of several plant species (Zhu et al., 2013; Yu et al., 2018, 2020; Xiao et al., 2021).

PE consists of four polysaccharide domains: homogalacturonan (HG), xylogalacturonan (XGA), rhamnogalacturonan I (RG-I), and rhamnogalacturonan II (RG-II). RG-I backbone is composed of GalA and Rha repeating units (Rha: GalA equals 1) (Renard et al., 1997). The RG-I sidechains are composed of single or numerous residues, and can be divided into arabinans, galactans and arabinogalactans type I and II (Voragen et al., 2009). Arabinans are composed of α-1,5-linked arabinose (Ara) units, and galactans are composed of β-1,4-linked galactose (Gal) residues (Atmodjo et al., 2013). HC consists of xyloglucans, xylans and mannans, and plays an important role in strengthening primary CWs by covalent and non-covalent interactions with cellulose and PE. These interactions are based on ester linkages and hydrogen bonds that are not stable under strong alkali conditions. Sequential alkali extraction is indeed necessary to degrade ester cross-links to extract HC1 and HC2 (Broxterman and Schols, 2018). Besides, RG-I sidechains are covalently and/or non-covalently linked to the xylan and xyloglucan (Broxterman and Schols, 2018), and can affect the viscosity and elasticity of the CW (Hwang et al., 1993; Kaczmarska et al., 2021).

Secondary CWs are primarily made up of cellulose, HC and lignin. Lignin is a highly cross-linked phenolic polymer of the secondary CW (Barberon et al., 2016). Lignification has been described as a strategy that plants use to immobilize Cd and as a tougher barrier for Cd entry (Parrotta et al., 2015; Loix et al., 2017).

Cellulose is the most rigid and inaccessible polysaccharide in the CW (Harris and Stone, 2009). Despite the abundance of hydroxyl groups in cellulose, raw cellulose has a poor adsorption and binding ability for trace metals (O'Connell et al., 2008; Ge et al., 2016).

In the present work, we aim to identify which CW components could be potentially involved in Cd hyperaccumulation or exclusion mechanisms in *A. halleri*. We analysed the ionomes, poly- and mono- saccharides composition, and glycan array of PL22-H and I16-E root CW. Furthermore, CW-related genes were selected based on previously published RNA-Seq data of PL22-H and I16-E (Corso et al., 2018), and glycan array results. Our results highlighted a major role for PE in Cd accumulation in *A. halleri* roots. Glycan array results showed a higher signal intensity of the pectic epitope (1→4)-β-galactan in I16-E than in PL22-H roots. Furthermore, the role of genes involved in galactan synthesis (*GALS* genes) and in other CW pathways in Cd exclusion and accumulation was further characterized by using corresponding *A. thaliana* mutants.

2. Materials and methods

2.1. Plant geographical origin and hydroponic culture

Arabidopsis halleri PL22-H and I16-E seeds were harvested in the south of Poland (Bukowno, 50°16'58.08"N, 19°28'43.38"E) and the

north of Italy (Val del Riso, 45°51'33.9"N, 9°52'35.3"E), respectively (Table S1; Fig. S1a; Corso et al., 2018; Schvartzman et al., 2018).

Hydroponic culture for *A. halleri* was performed according to Meyer et al. (2015) and Corso et al. (2018). PL22-H and I16-E seeds were germinated on soil. After 4 weeks of growth on soil, *A. halleri* plants were transferred to a modified Murashige and Skoog (MS) solution (Table S2; Meyer et al., 2015; Corso et al., 2018) for an additional 4 weeks. Then half of plants (15 plants per replicate, 3 repetitions) were treated with 5 μM $CdSO_4$, while the other half grown in the standard (control) solution for 10 days.

Hydroponic culture for *A. thaliana* plants was similar to that of *A. halleri*, except for the composition of the solution that was modified for Ca (1 mM Ca $(NO_3)_2$•4 H_2O) and Zn (1 μM $ZnSO_4$•7 H_2O) (Table S2). After three weeks of growth, half of the plants (5 plants per replicate, 3 repetitions) were treated with 2.5 μM $CdSO_4$ and the other half plants grown in the normal solution for 10 days.

After treatment, roots were washed with 0.5 mM $CaCl_2$ and H_2O for 10 min. Roots and shoots were wiped off with tissue paper before being weighed, frozen and homogenized into a fine powder with a mortar and pestle in liquid nitrogen before storage at – 80 ℃.

2.2. Arabidopsis halleri and Arabidopsis thaliana in vitro culture

Seeds were sterilized for 5 min in 75% Ethanol and 3 min in 20% bleach, then rinsed twice with sterile ddH_2O. Sterile seeds were sown on petri plates containing ½MS medium (containing 1% sucrose) and stored at 4 ℃ for 72 h. Plants then were vertically cultivated in the growth chamber (16 h: 8 h, light: dark, 22 ℃; 150 μmol light intensity). The plants were used for following experiments:

For the CW and lignin histological staining of *A. halleri*, seeds were sown on petri plates containing ½MS medium (containing 1% sucrose) for 5 days. Then seedlings were transferred to ½ MS or ½ MS + 50 μM $CdCl_2$ (5–7 seedlings per treatment) for another 5 days. Roots were harvested and cut into two zones: the root tip zone (0–1 cm) and the root mature zone (1–2 cm). The staining was performed according to Ursache et al. (2018). Calcofluor white and basic fuchsin were used to visualize the CW and lignin, respectively.

For the Cd tolerance measurement of *A. thaliana* plants, the seeds were sown on petri plates containing ½ MS medium (+ 1% sucrose) for 7 days. After that, the plants were transferred to ½ MS, ½ MS + 50 μM $CdCl_2$ and ½ MS + 75 μM $CdCl_2$ for another 7 days. Then the roots were scanned directly in the plates, while the shoots were tilled on a square glass and then scanned by the EPSON Perfection V30. The primary and lateral root length (PR and LR) and numbers of lateral roots (NLR) were analysed by ROOTNAV software (Pound et al., 2013), the shoot area (SA) was measured with FIJI software (Schindelin et al., 2012).

2.3. Root cell wall extraction and fractionation

The crude CWs of PL22-H and I16-E roots of plants cultivated in hydropony were fractionated into PE, hemicellulose 1 (HC1), and HC2 by following the method of Zhong and Lauchli (1993) with some modifications. Briefly, 0.5 g root powders were homogenized in 10 ml of ice-cold 75% Ethanol for 20 min, and then the supernatant was discarded following centrifugation (10 min, 8000 g, 4 ℃). The pellets were homogenized and washed with 7 ml of ice-cold acetone (twice), methanol: chloroform (1:1) (twice) and methanol (twice). The supernatant was removed after centrifugation (10 min, 8000 g, 4 ℃) between wash steps. The final powders named "CW material" were freeze-dried overnight and kept at 4 ℃. PE was extracted from 35 mg of dry CW materials using 3 ml of 0.5% ammonium oxalate buffer containing 0.1% $NaBH_4$ in 95 ℃ water-bath for 1 h. Samples were centrifuged 10 min at 1,3800 g and the supernatant was collected. The procedure was repeated twice and the two supernatants were combined. After being washed twice with ddH_2O, the pellet was utilized for HC1 extraction. HC1 was extracted twice by 3 ml 4% NaOH containing 0.1% $NaBH_4$ at room temperature for 24 h totally, the supernatants are HC1. HC2 has followed the same method but with 24% NaOH containing 0.1% $NaBH_4$.

2.4. Quantification of pectin and hemicellulose contents

The uronic acid content of the PE fraction was measured according to Blumenkrantz and Asboe-Hansen (1973). Briefly, 100 μl extracts were incubated in glass tubes with 500 μl 98% H_2SO_4 containing 0.0125 M $Na_2B_4O_7$·10 H_2O for 5 min at 100 ℃. After cooling, 10 μl of m-Hydroxydiphenyl (0.15%) was added and after 20 min incubation at room temperature, the absorbance at 520 nm was measured using the BioTek Gen5 Plate Reader (BioTek, USA). Galacturonic acid (Sigma) was used to construct the calibration curve. Total polysaccharide contents of HC1 and HC2 fractions were measured according to the phenol sulfuric acid method of Dubois et al. (1956) and Shi et al. (2015). Briefly, 100 μl extracts were firstly incubated with 500 μl 98% H_2SO_4 and 5 μl 80% phenol in glass tubes at room temperature for 15 min, then were incubated at 100 ℃ for another 15 min. After cooling, the absorbance at 490 nm was measured by the BioTek Gen5 Plate Reader (BioTek, USA). Glucose was used to construct the calibration curve.

2.5. Quantification of monosaccharides of root cell walls

Root samples were homogenized at 80 ℃ in 96% Ethanol for 15 min (twice), acetone for 15 min (at room temperature). During each step of homogenization, the supernatants were removed after centrifugation (5 min, 10,000 g) and the final pellets (CW extractions) were dried overnight. Quantification of monosaccharides was performed by gas chromatography-mass spectrometry (GC-MS) in a combination of methoximation followed by trime-thylsilylation (TMS) derivatization (MeOx_TMS) method according to Yi et al. (2014). The molar ratio Gal: Rha and (Ara + Gal): Rha was used to determine the lengths of RG-I galactan and arabinogalactan sidechains, respectively. Since the backbone of PEs is composed of HG (100% GalA) and RG-I, the PE structure modification was determined by the HG: RG-I molar ratio which is calculated as the molar ratio of (GalA-Rha): (2 ×Rha) (Huang et al., 2017).

2.6. Lignin quantification

Lignin was extracted from PL22-H and I16-E roots of plants cultivated in hydroponics following the method of Wang et al. (2018) with some modifications. Briefly, 100 mg of the root powder was washed with 3 ml 50 mM potassium phosphate buffer (pH=7.0) (twice), 1% Triton X-100 (twice), 1 M NaCl (twice), ddH_2O (twice) and 80% acetone (twice). Samples were centrifuged at 3000 g for 15 min and the supernatant was discarded. The pellet was freeze-dried overnight. Around 3–5 mg CW dry samples were incubated with 200 μl thioglycolic acid and 1 ml of 2 M HCl at 95 ℃ for 4 h. After cooling, the supernatant was discarded after 15 min of centrifugation at 12,000 rpm, while the pellet was washed three times with 1 ml ddH_2O. The pellet was then incubated overnight at 4 ℃ in 600 μl 0.5 M NaOH on a shaker (300 rpm). The supernatant was collected in 1.5 ml tube after 15 min of centrifugation at 5000 rpm, and the pellet was extracted with another 600 μl 0.5 M NaOH for 1 h as before. Then the supernatants from two extractions were combined and incubated with 240 μl concentrated HCl for 4 h at 4 ℃. The pellet was collected after centrifugation at 12,000 rpm for 10 min and was then dissolved in 1800 μl 0.5 M NaOH. The absorbance was measured with a Bio-Rad SmartSpec Plus UV/Vis Spectrophotometer at 280 nm using quartz cuvettes.

2.7. Cell wall glycan -Comprehensive Microarray Polymer Profiling (CoMPP)

Alcohol Insoluble Residue (AIR) of root powder (10 mg) was prepared according to Moller et al. (2012). The PE and HCs were

sequentially extracted from AIR samples using 30 µl 50 mM Cyclohexane Diamine Tetraacetic Acid (CDTA) and 30 µl 4 M NaOH in 0.1% $NaBH_4$ (w/v). Extracted samples were then diluted at four concentrations with 10x glycerol buffer (47% glycerol, 0.06% Triton, 0.04% Proclin 200) and then were printed (two technical replicates) to nitrocellulose membrane using a Sprint micro-array robot (Arrayjet, Roslin, UK). Arrays were firstly blocked using 5% milk protein in TBS buffer with 0.1% Tween-20 (v/v, MP-TBST), and then were probed with rat conjugated primary antibodies (1:10 in MP-TBST buffer dilution, Plant Probes) for 1.5 h. Arrays were then washed with TBST (15 min, 3 times). Afterwards, arrays were probed with the anti-rat alkaline phosphatase secondary antibody (1:200 MP-TBST dilution, Sigma), and then washed with ddH_2O (15 min, 3 times), and finally stained using NBT/BCIP standard protocol (Sigma). Probed arrays were scanned using a Canon 9000 F MarkII flatbed scanner (2400 DPI) and images were analysed with Array-Pro Analyzer (v.6.3.1) and Image J. These images were used to generate spot signal values for producing a heatmap integrated with hierarchical clustering.

2.8. Mineral element analysis

For the measurement of micro-elements in CW components, the PE and HC1 extracts (3 ml) were digested with 7 ml of 7 N HNO_3 for 6 h at 120 °C. For the mineral elements measurement of shoots and roots of *A. halleri* and *A. thaliana* plants grown in hydroponic solution, roots and shoots were dried at 55 °C until constant weight. Aliquots of 50 mg dried materials were digested with 10 ml of 7 N HNO_3 for 6 h at 120 °C. Total Cd, Zn, Fe, Ca and Mn were measured after dilution using microwave plasma atomic emission spectrometers (MP-AES 4200; Agilent Technologies). Certified standard samples were used to prepare the quality control solution.

2.9. RNA extraction and Quantitative Real-Time PCR (qRT-PCR)

Total RNA was extracted from 100 mg of *A. halleri* and *A. thaliana* roots grown in hydroponics using the Maxwell® LEV Plant RNA Kit (www.promega.com, Promega, Madison, WI, USA). RNA was quantified with the Nano Drop 2000 UV-Vis Spectrophotometer (Thermo Scientific, Loughborough, UK). 1 µg of total RNA was used for cDNA synthesis using the Go Script™ Reverse Transcriptase kit (Promega). The cDNA was used for qRT-PCR using the Go Taq® qPCR and RT-qPCR Systems kit (Promega). *SHR* was used as reference gene in *A. halleri*. *CKIIα* and *CDTA* were used as the reference genes in *A. thaliana*. Relative quantification of Livak method was used to analyse and represent the data. The relative quantification of these genes was calculated by three technical replicates and three biological replicates. Primers used in this study are listed in Table S3.

2.10. Selection of root cell wall-related genes in A. halleri and corresponding mutants in A. thaliana

In a previous study, Corso et al. (2018) identified 233 root CW-related differentially expressed genes (DEGs) between PL22-H and I16-E roots grown in control condition or subjected to Cd treatment. In this work, genes were selected from the same dataset by filtering transcripts showing $\log_2$ PL22-H / I16-E gene expression < -1 or > 1. CW-genes were selected based on the glycan array results, and by screening Wallprot database (San Clemente and Jamet, 2015), AgriGo database (Tian et al., 2017) and published literature. The description of selected genes can be found in Table 1 and Table S4.

Arabidopsis thaliana wild-type (WT), T-DNA insertion mutants and the *GALS1* overexpressing line were in the Columbia-0 (Col-0) background. The T-DNA insertion mutants *GALACTAN SYNTHASE 1* (*GALS1; gals1–1* SALK_016687c, *gals1–2* WiscDsLox443D3*)* and *GALS1-overexpressing* line (*OE-GALS1#*5) were kindly provided by Prof. AYing Zhang and Dr Yan Jingwei (Nanjing Agricultural University, China). The other mutants in the genes *GALACTAN SYNTHASE 2* (*gals2 mutant*), *GALACTAN SYNTHASE 3* (*gals3 mutant*), *BIIDXI* (*bdx* mutant)*, LEUNIG_HOMOLOG* (*luh* mutant), *ARABINAN DEFICIENT 2* (*arad2* mutant), *PECTIN METHYLESTERASE 18* (*pmei18* mutant), *LEUCINE_RICH REPEAT EXTENSIN 10* (*lrx10* mutant)*, PEPTIDOGLYCAN-BINDING LYSM DOMAIN CONTAINING-PROTEIN* (*lysm* mutant), *ASPARTYL PROTEASE FAMILY 2* (*apf2* mutant), *WATER SOLUBLE CHLOROPHYLL-BINDING PROTEINS* (*wscp* mutant), *CHITINASE* (*chitinase* mutant) and *PEROXIDASE SUPER FAMILY PROTEIN 39* (*per39* mutant) were ordered from the Nottingham Arabidopsis Stock Centre (NASC). To obtain the homozygous *KO* mutants, seeds were selected on MS medium with the indicated antibiotic and were genotyped by PCR. The genes and relative primers are listed in Table S5.

2.11. Statistical analysis

The statistical analyses were carried out with GraphPad Prism 8.1 software by i) one-way ANOVA with Tukey's range test (among *A. halleri* populations and conditions; $P < 0.05$) and ii) two-tailed t-test (*A. thaliana* wild-type vs mutants; $P < 0.05$).

Table 1
List of root CW-related genes and corresponding mutants.

Name	Full name	AGI	T-DNA	Function description
CHITINASE	*CHITINASE*	AT2G43620	SALK_056680c	Poly-beta-glucosaminidase
PER39	*PEROXIDASE SUPER FAMILY PROTEIN 39*	AT4G11290	SALK_096147c	Oxido-reductase involved in lignin polymerization
APF2	*ASPARTYL PROTEASE FAMILY 2*	AT1G01300	SALK_021485c	Protease
WSCP	*WATER SOLUBLE CHLOROPHYLL-BINDING PROTEINS*	AT1G72290	SALK_009681	Interaction with other proteins or polysaccharides
LysM	*PEPTIDOGLYCAN-BINDING LYSM DOMAIN CONTAINING-PROTEIN*	AT5G23130	SALK_111440c	Interaction with other proteins or polysaccharides
LRX10	LEUCINE_RICH REPEAT EXTENSIN 10	AT2G15880	SALK_087083c	Structural protein
PMEI18	*PECTIN METHYLESTERASE 18*	AT1G11580	SALK_031903c	Pectin methylesterase inhibitor
BDX	*BIIDXI*	AT4G32460	SALK_037090c	Involved in pectin methyl esterase regulation
LUH	*LEUNIG_HOMOLOG*	AT2G32700	SALK_107245c	a Groucho/TUP1 transcriptional co-repressor, regulating pectin modification
ARAD2	*ARABINAN DEFICIENT 2*	AT5G44930	SALK_205745c	Arabinosyltransderase
GALS1–1	*GALACTAN SYNTHASE 1*	AT2G33570	SALK_016687c	Glycosyltransferase
GALS1–2		AT2G33570	WiscDsLox443D3	
GALS2	*GALACTAN SYNTHASE 2*	AT5G44670	SALK_121391c	
GALS3	*GALACTAN SYNTHASE 3*	AT4G20170	Wisc_DsLox377–380G11.0	
*OE-GALS1#*5	*GALACTAN SYNTHASE 1*			

3. Results

3.1. Cd tolerance and accumulation in roots and root cell wall polysaccharides

Fresh biomass, chlorophyll content and Cd concentration were analysed in PL22-H and I16-E plants grown in hydroponics and treated for 10 days with 5 μM Cd, which corresponded to a realistic concentration (0.6 ppm; Meyer et al., 2015; Corso et al., 2018; Corso et al., 2021) and was reported as the median toxic concentration for plants grown in solutions (Kopittke et al., 2010). Although some PL22-H plants exhibited chlorosis symptoms (Fig. S1b), no significant differences in chlorophyll content or biomass were observed between PL22-H and I16-E (Fig. S1c, d). In addition, I16-E showed a significantly lower Cd concentration in the shoots than PL22-H (as in Corso et al., 2018; Fig. S2a). Analysis of the mineral profile (Fig. S2b, c, d) highlighted that the Cd and Zn translocation factors (TFs), i.e. the ratio between concentrations in shoots and roots, were at least two-fold higher in PL22-H than I16-E (Fig. S2d).

Taken together, these results confirmed that PL22-H and I16-E adopt different strategies to cope with Cd addition in the medium (Meyer et al., 2015; Corso et al., 2018). In addition, Corso et al. (2018) showed that several root CW-related DEGs showed constitutive and higher expression in I16-E than in PL22-H. Thus, we hypothesize that difference in the Cd accumulation between PL22-H and I16-E shoots was due at least partially to root CW components that could affect Cd moving in the root and/or Cd translocation from roots to shoots.

Analyses of the PE and HC extracted from the root CWs highlighted a higher concentration of Cd in PE than in the HC1 fraction, i.e. 10 times more in PL22-H and 3 times more in I16-E root PE compared to HC1 (Fig. 1a). Furthermore, the PE fraction contained a three-fold higher concentration of Cd in PL22-H than in I16-E roots, while no difference in Cd concentration was observed between these two populations in the HC1 fraction (Fig. 1a).

3.2. Quantification of pectin and hemicellulose contents, and monosaccharides compositions of PL22-H and I16-E root cell walls

PE and HC1 showed contrasting Cd accumulation in PL22-H and I16-E (Fig. 1a). Hence, The PE and HC compositions were further analysed by characterizing the uronic acid in the PE and the total sugar in HC polysaccharides. Since Cd hyperaccumulation mechanisms are constitutively activated in PL22-H and I16-E *A. halleri* populations, the PE and HC contents were measured in both control and Cd treatment conditions. The PE content was comparable in both control and Cd-treated PL22-H and I16-E root CWs (Fig. 1b). On the contrary, The HC content was 1.7-fold higher in I16-E than PL22-H upon Cd exposure, whereas it was similar in the control condition (Fig. 1c). After Cd treatment, the ratio of the HC2 to HC1 dropped sharply in both PL22-H and I16-E (Fig. 1d). The monosaccharides in root CWs were further characterized in PL22-H and I16-E roots (Fig. 2a). PL22-H contained higher glucose and lower fucose contents compared to I16-E under Cd condition, while no difference was observed in control condition (Fig. 2a). Moreover, Cd treatment shortened by 14% the RG-I galactan sidechain and 19% the arabinogalactan sidechain in PL22-H, while no changes were observed for I16-E (Fig. 2b). Interestingly, Cd treatment

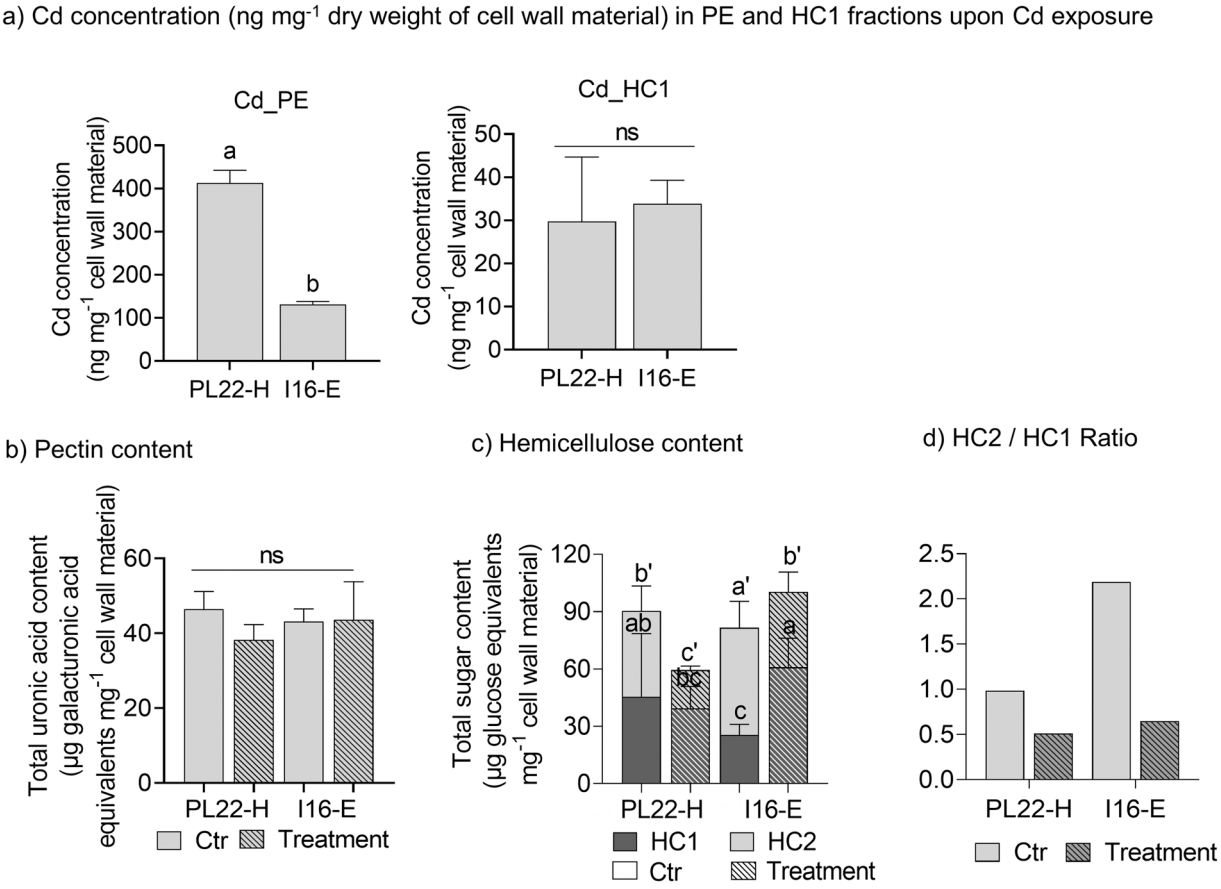

Fig. 1. Pectin and hemicellulose content and their ability to retain Cd in PL22-H and I16-E roots. a) Cd concentrations in PE and HC1 fractions. b, c) PE (b) and HC (c) content in root CW of PL22-H and I16-E in control and Cd treatment conditions. d) HC2 / HC1 ratio in PL22-H and I16-E grown in control and Cd treatment conditions. Different letters indicate statistically significant differences ($P < 0.05$) assessed by ANOVA with Tukey's range test. ns = not significant. Error bars represent the standard deviation (3 biological repetitions). a, a' letters indicate statistically significant differences among HC1 and HC2 polysaccharides.

a) Monosaccharide compositions of cell wall carbohydrates of PL22-H and I16-E roots

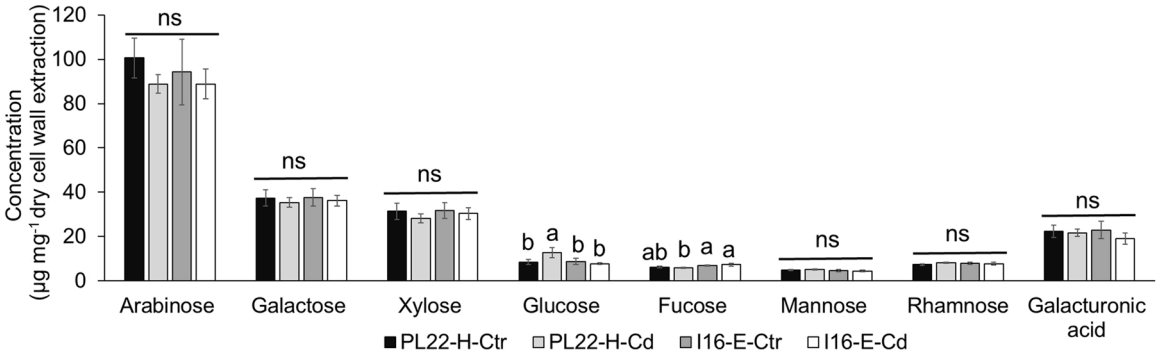

b) RG-I sidechain length and pectin structure modification

RG-I galactan sidechain length	PL22-H	I16-E
Ctr	5.15	4.76
Cd treatment	4.38	4.70
Percentage Cd/Ctr	85.16	98.79

Arabinogalactan sidechain length	PL22-H	I16-E
Ctr	18.99	16.67
Cd treatment	15.42	16.24
Percentage Cd/Ctr	81.21	97.38

Pectin structure modification	PL22-H	I16-E
Ctr	1.04	0.95
Cd treatment	0.85	0.74
Percentage Cd/Ctr	81.76	78.27

c) Lignin content in PL22-H and I16-E root cell walls

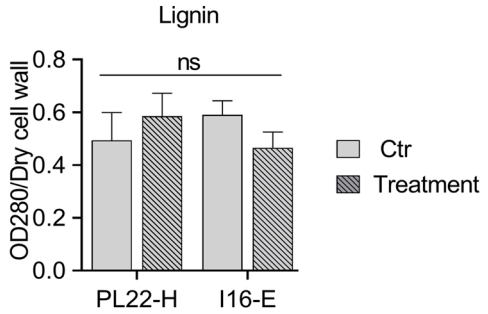

d) *A. halleri* differentially expressed genes related to lignin synthesis

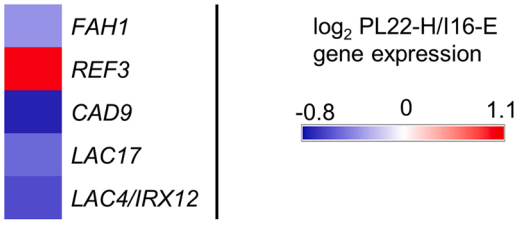

Fig. 2. Monosaccharides and lignin analysis in PL22-H and I16-E roots. a) Monosaccharides composition of PL22-H and I16-E roots grown in control and Cd treatment conditions. b) RG-I galactan and arabinogalactan sidechain length and PE structure modification (HG: RG-I). c) Lignin content expressed by the OD_{280} per dry CW materials of PL22-H and I16-E grown in control and Cd treatment conditions. d) Differentially expressed lignin-related genes ($P < 0.05$) between PL22-H and I16-E roots. Red and blue colours indicate genes that showed higher and lower expressed in PL22-H than I16-E, respectively. Different letters indicate statistically significant differences ($P < 0.05$) assessed by ANOVA with Tukey's range test. ns = not significant. Error bars represent the standard deviation (3 biological repetitions).

induced PE structure modification (HG: RG-I) in both PL22-H and I16-E (Fig. 2b). Interestingly, Cd treatment induced PE structure modification (HG: RG-I) in both PL22-H and I16-E (Fig. 2b).

3.3. Analysis of lignin content and distribution in PL22-H and I16-E roots

The potential role of secondary CW on Cd accumulation was also investigated by measuring lignin content, distribution, and analysing the expression of lignin biosynthetic genes in PL22-H and I16-E roots (Fig. 2c, d; S4a, b; Corso et al., 2018). Although lignin concentration showed no significant difference between PL22-H and I16-E roots both in control and Cd conditions (Fig. 2c), some genes involved in lignin biosynthesis (Fig. S3; Dixon and Barros, 2019), i.e. *CINNAMYL ALCOHOL DEHYDROGENASE 9* (*CAD9*), *FERULATE-5-HYDROXYLASE* 1 (*FAH1*), *LACCASE4* and *17* (*LAC4 and LAC17)* showed significantly higher expression in I16-E than PL22-H (Fig. 2d).

In addition, lignin distribution in the root tip and mature zone of 14-day-old PL22-H and I16-E seedlings was analysed by histological staining. Similar lignin distribution was observed in the root tip and mature zone between the two populations (Fig. S4a, b). No difference was observed between the root diameters of the two populations (Fig. S4c).

3.4. Analysis of epitopes of cell wall polysaccharides and relative gene expression in PL22-H and I16-E roots

CW glycan profiles were characterized in the PE and HC root fractions of PL22-H and I16-E via the CoMPP technique, by using 20 antibodies raised against specific CW components (Moller et al., 2007).

Compared to the control condition, the signal intensities of most PE epitopes decreased upon Cd exposure (Fig. 3). Conversely, the signal intensities of most HC epitopes increased upon Cd treatment in PL22-H but did not show differences with I16-E. In particular, Cd reduced the signal intensity of LM15, CCRC-M87 and LM21 in I16-E, whereas they did not show major differences between Cd and control in PL22-H. The signal intensities of LM10 and LM11 increased upon Cd in PL22-H, while they showed no difference between control and Cd in I16-E (Fig. 3).

Most CW epitopes showed higher relative abundance in I16-E compared to PL22-H in the control condition. In particular, (1→5)-α-arabinan (recognized by LM6 mAb) and (1→4)-β-galactan (recognized by LM5 mAb) of the PE fraction showed the largest difference in signal intensities between PL22-H and I16-E roots in the control condition, followed by arabinogalactan protein (recognized by JIM13 mAb and LM2 mAb) (Fig. 3). The same was true for the HC domains of non-fucosylated xyloglucan (recognized by LM15 mAb), β-linked mannan polysaccharides (recognized by LM21 mAb) and xyloglucan oligosaccharides (recognized by CCRC-M87 mAb) (Fig. 3).

Data presented in this study showed that I16-E exhibited a considerably lower Cd concentration than PL22-H in the PE fraction (Fig. 1a), and LM5 and LM6 mAbs showed higher signal intensities in I16-E compared to PL22-H (Fig. 3). We therefore hypothesized that (1→5)-α-arabinan and (1→4)-β-galactan may be involved in limiting Cd translocation from roots to shoots. In addition, the expression values of *ARAD2* and *GALS1* that are involved in the synthesis of (1→5)-α-arabinan and (1→4)-β-galactan (Harholt et al., 2012; Liwanag et al., 2012), respectively, were extracted from the published RNA-Seq data on I16-E and PL22-H roots (Corso et al., 2018, Fig. S5a) and further confirmed by qRT-PCR (Fig. 4a). Both genes showed a higher expression in I16-E compared to PL22-H in control and Cd-treatment conditions.

3.5. Characterisation of A. thaliana mutants affected in (1→5)-α-arabinan and (1→4)-β-galactan synthesis

Cd tolerance and Cd accumulation were analysed in *A. thaliana* mutants for genes involved in (1→5)-α-arabinan synthesis, i.e. *arad2*, and (1→4)-β-galactan synthesis, i.e. *gals1, gals2, gals3* and *GALS1* overexpressor (*OE-GALS1#5*; Fig. 4b, c, d, e, f). Based on preliminary data obtained and previous publications (Meyer et al., 2015; Corso et al., 2018), 50 μM and 75 μM Cd were selected to test Cd tolerance in vitro. In the control condition, *arad2* plants showed a significantly longer primary root length and a larger shoot area than the WT, and *gals1–1, gals2, gals3* and *OE-GALS1#5* showed significantly longer lateral root lengths than WT (Fig. 4c). Upon Cd treatments, *arad2* had significantly shorter lateral root lengths than WT, indicating a higher sensitivity to Cd. On the contrary, the primary root growth of *gals1–1* and *gals2* mutants was less affected than the WT and the shoot growth of *OE-GALS1#5* plants was significantly less inhibited than WT, suggesting a higher tolerance to Cd than WT (Fig. 4c).

Ionomic analysis showed that Cd accumulation in *arad2* roots and shoots was similar to the WT (Fig. 4d, e). The *gals1–1, gals2, gals3* and *OE-GALS1#5* mutants accumulated more Cd than the WT in the shoots (Fig. 4d), and similar Cd concentration compared to the WT in the roots (Fig. 4e). Both *gals1–1* and *OE-GALS1#5* mutants showed higher Cd root-to-shoot translocation than WT (Fig. 4 f). Other metal accumulation and TF were also affected. Zn accumulated significantly more in the shoots of all *GALS* loss and gain-of-function mutants (Fig. 4d), which

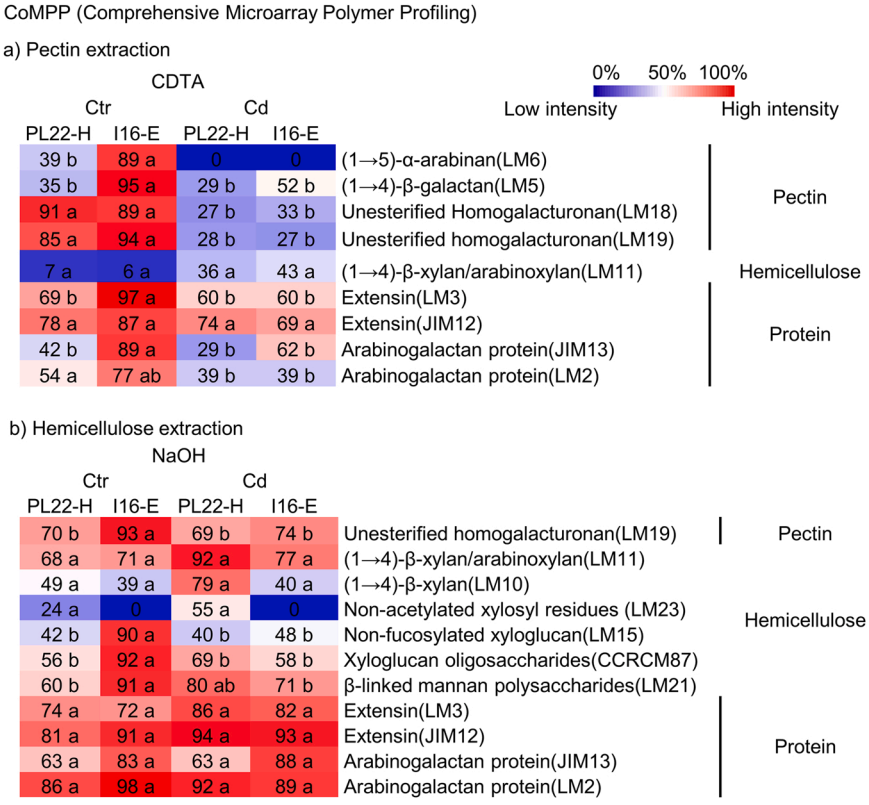

Fig. 3. Glycan array of PL22-H and I16-E pectin and hemicellulose in roots. a, b) Signal intensities of CW polysaccharides' epitopes in CDTA extracted PE (a) and NaOH extracted HC (b) fractions. The quantities are calculated as percentages related to the sample showing the highest accumulation value for each antibody (100%, 50% and 0% for red, white and blue colour, respectively) within I16-E and PL22-H. LM = Leeds monoclonal antibodies, JIM = John Innes monoclonal antibodies. Different letters indicate statistically significant differences ($P < 0.05$) assessed by ANOVA with Tukey's range test (3 biological repetitions).

a) Relative expression levels of *GALS1* and *ARAD2* genes normalized to the *SHR* reference gene

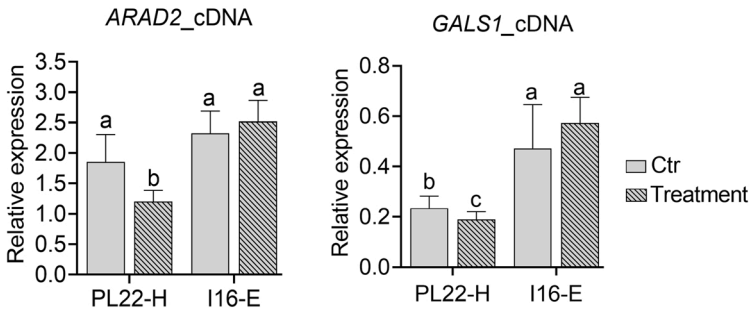

b) Picture of seedlings grown upon 50 µM Cd treatment

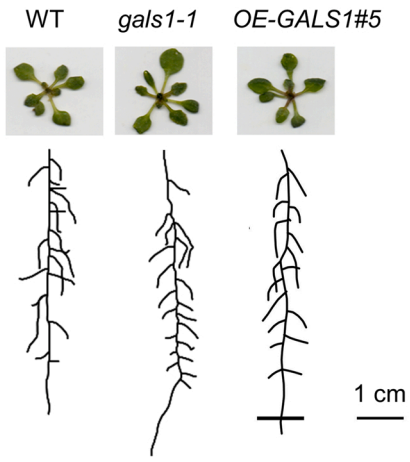

c) Summary of physiological analyses of *arad2* and *gals* mutants

Condition	Para-meters	*arad2*	*gals1-1*	*gals1-2*	*gals2*	*gals3*	*OE-GALS1#5*
Ctr	PR	*		*			*
Ctr	LR		*		*	*	*
Ctr	NLR	*					
Ctr	SA	*			*	*	
50µM	PR		*	*	*		
50µM	LR				*		*
50µM	NLR					*	
50µM	SA		*				*
75µM	PR		*	*	*		
75µM	LR	*	*				*
75µM	NLR			*		*	*
75µM	SA						*

d) Mineral profile of the aerial parts of mutants
Relative values compared with WT (%)

Shoot	*arad2*	*gals1-1*	*gals1-2*	*gals2*	*gals3*	*OE GALS1#5*
Cd	111	131*	107	127*	124*	123*
Zn	114*	129*	111*	123*	116*	125*
Mn	121*	119*	118*	118	104	114

e) Mineral profile of the roots of mutants
Relative values compared with WT (%)

Root	*arad2*	*gals1-1*	*gals1-2*	*gals2*	*gals3*	*OE GALS1#5*
Cd	117	109	109	112	115	102
Zn	101	103	109	108	114	103
Mn	109	100	82	87	97	93

f) Metal translocation factors of mutants
Relative values compared with WT (%)

Metal TF	*arad2*	*gals1-1*	*gals1-2*	*gals2*	*gals3*	*OE GALS1#5*
Cd	95	120	98	113	107	120
Zn	113	125	102	114	102	122
Mn	111	119	144	136	108	123

45% 100% 155%
(%) mutant / wildtype

Fig. 4. *ARAD2* and *GALS1* expression levels in *A. halleri* and characterization of the corresponding *A. thaliana* mutants. a) Relative *ARAD2* and *GALS1* expression levels in *A. halleri*. b) Picture of *gals1*, *OE-GALS1#5* and WT seedling grown with 50 µM Cd. c) Summary of physiological analyses of mutants grown in control or upon Cd treatment. Primary root length (PR), lateral root length (LR), number of lateral root length (NLR) and shoot area (SA) are shown. Plantlets were grown in control condition or subjected to 50 µM and 75 µM Cd treatment for 7 days. d, e, f) Concentrations of mineral elements in shoots (d) and roots (e), and metal translocation factors (f) of plants grown in hydroponics and treated with 2.5 µM Cd for 10 days. The translocation factor was evaluated from the ratio of mineral element in shoot to that in root. Physiological analyses and concentrations of mineral elements are relative values (in %) with respect to WT. Asterisks indicate

statistically significant differences ($P < 0.05$) assessed by two-tailed t-test of mutants compared with WT. Error bars represent the standard deviation (3 biological repetitions).

also increased the TF compared with the WT (Fig. 4 f). Mn accumulated significantly more in the shoots of *gals1–1* and *gals1–2* and its translocation was increased in most of all *gals* and *OE-GALS1#5* mutants.

Because of the phenotype similarity, the expression of *GALS1* and the monosaccharide profile was analysed in the roots of *gals1–1* and *OE-GALS1#5* roots. *GALS1* was more expressed in *OE-GALS1#5* compared to WT, while its expression was not detectable in the *gals1–1* mutant (Fig. S5b). The monosaccharide contents of *gals1–1* roots were similar to the WT (Fig. 5a), but a higher galactose content in *OE-GALS1#5* roots compared to WT was measured both in control and Cd conditions (Fig. 5a). However, Cd induced a significant reduction of GalA content in *OE-GALS1#5* roots (Fig. 5a). Furthermore, *gals1–1* and *OE-GALS1#5* showed longer RG-I galactan and arabinogalactan sidechains after Cd treatment, and *OE-GALS1#5* also showed a modification in the PE structure (HG: RG-I) (Fig. 5b).

3.6. Screening of cell wall-related Arabidopsis thaliana mutants

Besides *ARAD2* and *GALS1*, other CW-related DEGs between PL22-H and I16-E roots were identified (Fig. 6a) based on previously published RNA-Seq analysis (Fig. S5c; Corso et al., 2018), and the corresponding mutants were characterized for Cd tolerance and accumulation. These genes are involved in PE methyl esterification (*PMEI18, LUH, BDX*) and other CW-related pathways (*LRX10, LYSM, APF2, WSCP, CHITINASE, PER39*) (Table 1, S4).

Based on in vitro growth analyses of *A. thaliana* seedlings (Fig. 6b), *luh, bdx, lysm* and *lrx10* showed similar root and shoot growth compared to WT in the control condition. Among them, *lysm and bdx* had significantly shorter primary root lengths than WT upon Cd exposure. On the contrary, *luh* showed significantly longer lateral root lengths than WT upon Cd exposure, suggesting it was more Cd tolerant than WT. Mineral elements analysis of plants grown in hydroponics highlighted that *per39*, *luh* and *bdx* mutants accumulated significantly more Cd than WT in roots (Fig. 6c), and that *per39, pmei18* and *luh* mutants accumulated significantly more Cd than WT in shoots (Fig. 6d). Nevertheless, the Cd translocation factor of mutants and WT were similar (Fig. 6e). It is interesting to note that *pmei18* and *prx39* mutants were also affected in Zn and Mn accumulation in the roots and shoots, and *luh* mutant showed a 1.45 higher Zn translocation factor than WT (Fig. 6c, d).

4. Discussion

In this work, biochemical, genetics and molecular analyses were performed to characterize the potential role of root CW composition in variable Cd accumulation of *A. halleri*. In addition, physiological analyses were performed on galactan and other CW-related mutants to analyse the role of the corresponding genes in Cd tolerance and Cd accumulation in *A. thaliana*.

a) Monosaccharide compositions of root cell wall carbohydrates of galactan synthesis-related mutants

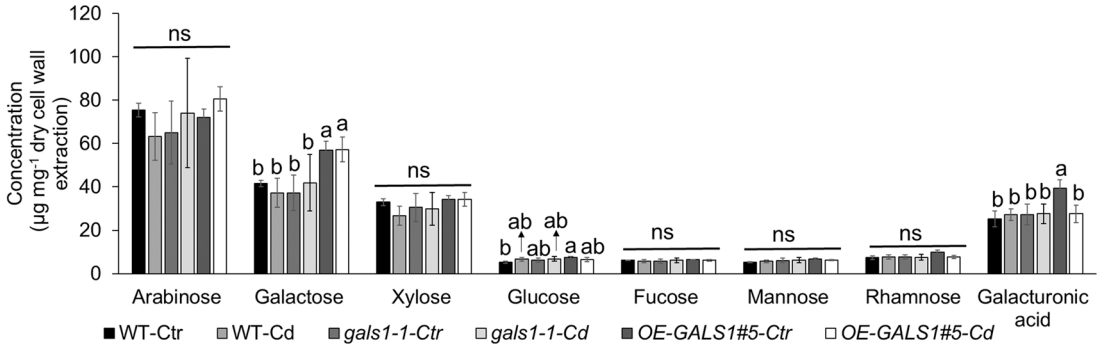

b) RG-I sidechain length and pectin structure modification in the roots

RG-I galactan sidechain length	WT	*gals1-1*	*OE-GALS1#5*
Ctr	5.66	4.84	5.68
Cd treatment	4.90	5.55	7.47
Percentage Cd Ctr^{-1}	86.61	114.61	131.50

Arabinogalactan sidechain length	WT	*gals1-1*	*OE-GALS1#5*
Ctr	15.94	13.29	12.89
Cd treatment	13.23	15.35	17.99
Percentage Cd Ctr^{-1}	83.01	115.49	139.56

Pectin structure modification	WT	*gals1-1*	*OE-GALS1#5*
Ctr	1.22	1.27	1.47
Cd treatment	1.29	1.33	1.30
Percentage Cd Ctr^{-1}	105.64	104.32	88.56

Fig. 5. Monosaccharides analysis of *gals1–1* and *OE-GALS1#5* roots for plants grown in hydroponics. a) Quantification of monosaccharides in the roots. Different letters indicate statistically significant differences ($P < 0.05$) assessed by one-way with Tukey's range test. ns = not significant. Error bars represent the standard deviation (3 biological repetitions). b) RG-I sidechains length and modification of pectin structure in the roots. Plants were grown in hydroponics and treated with 2.5 µM Cd for 10 days.

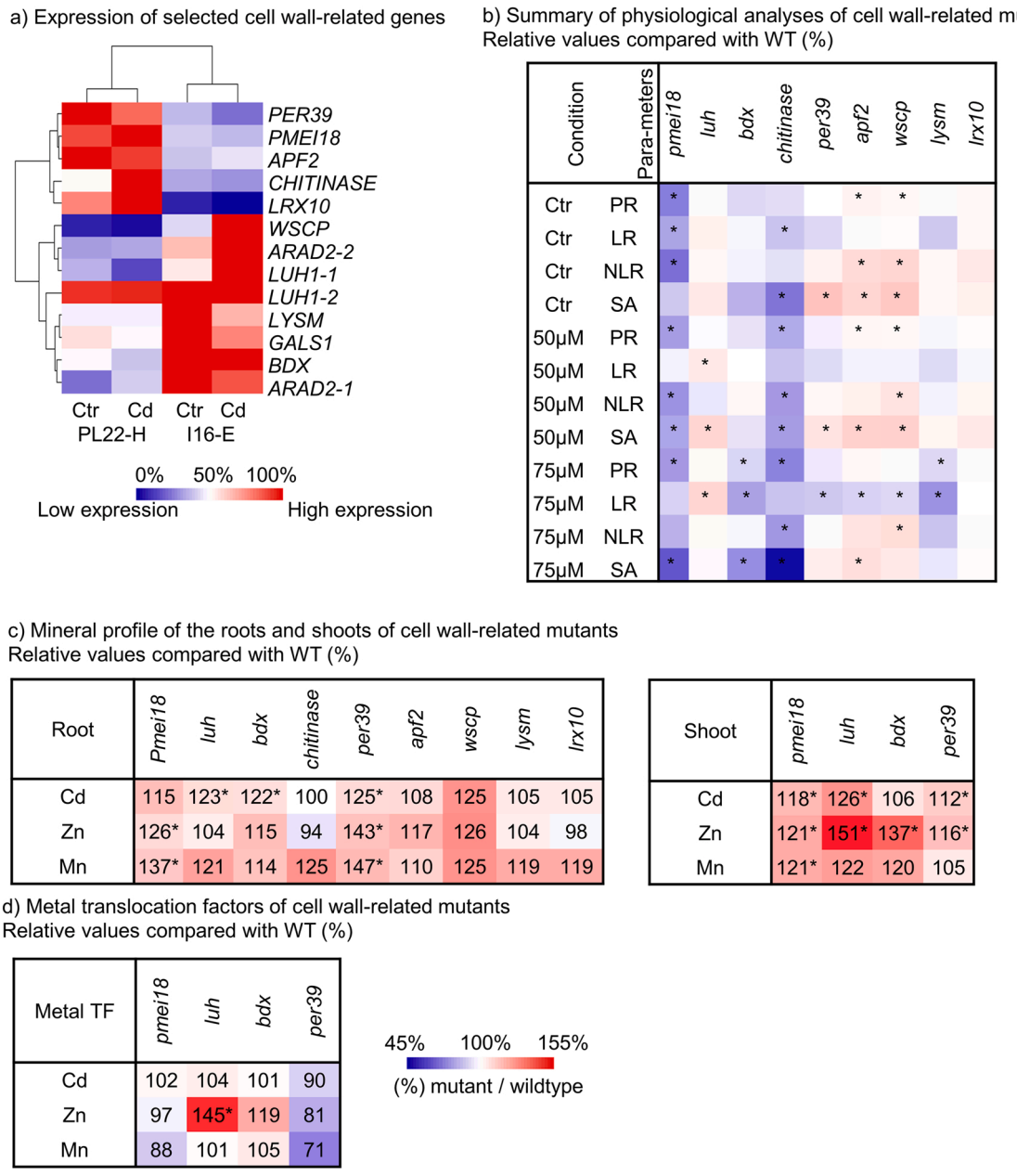

Fig. 6. Selection of cell wall-related genes and characterization of corresponding *A. thaliana* mutants. a) Expression of root CW-related differentially expressed genes between PL22-H and I16-E roots. Heatmap showing the RNA sequence (RNA-Seq) expression of CW-related genes that showed higher expression in PL22-H (log2 PL22-H/I16-E gene expression > 1) and I16-E (log2 PL22-H/I16-E gene expression < −1) in roots. The expression values are calculated as a percentage related to the sample showing the highest expression value for each gene (100%, 50% and 0% for red, white and blue colour, respectively) within I16-E and PL22-H (control (Ctr) and cadmium (Cd)). b) Summary of physiological analyses of CW-related mutants grown in control or upon Cd treatment. Primary root length (PR), lateral root length (LR), number of lateral root length (NLR) and shoot area (SA) of plantlets grown in control or upon 50 μM and 75 μM Cd treatment for 7 days. c, d) Concentrations of mineral elements in roots and shoots (c), and metal translocation factors (d) of plants grown in hydroponics and treated with 2.5 μM Cd for 10 days. The translocation factor was evaluated from the ratio of mineral element in shoot to that in root. Physiological analyses and concentration of mineral elements are relative values (in %) with respect to WT. Asterisks indicate statistically significant differences ($P < 0.05$) assessed by two-tailed t-test of mutants compared with WT (3 biological repetitions).

4.1. Pectin and hemicellulose influence Cd and Zn retention capacities in PL22-H and I16-E roots

Previous grafting experiments in tobacco, eggplant, and *Noccaea caerulescens* demonstrated that Cd concentration in shoots was, at first, controlled by root properties (Wagner, 1988; Arao et al., 2008; Guimarães et al., 2009). Similarly to what has been shown for *A. halleri* in this work (Fig. 1), published data on *Brassica chinensis* [pakchoi] (Wang et al., 2020), *Glycine max* [soybean] (Wang et al., 2018), *Oryza sativa L.* [rice] (Yu et al., 2020) and *Sedum alfredii* (Guo et al., 2020) demonstrated that CW-bound Cd was mainly accumulated in the PE and HC1 in plant roots. Results obtained in this work showed that Cd, Zn, Mn and Fe were more concentrated in the PE fraction of *A. halleri* root CW compared to HC1 (Fig. 1a; Fig. 7a, b), which highlighted a key role of the PE in TMs accumulation. In addition, this study showed that the PE from root CW exhibited a higher Cd but a lower Zn retention capacity in PL22-H than in I16-E (Fig. 1a; Fig. 7a), suggesting different PE metal binding properties between the two populations. This result was in

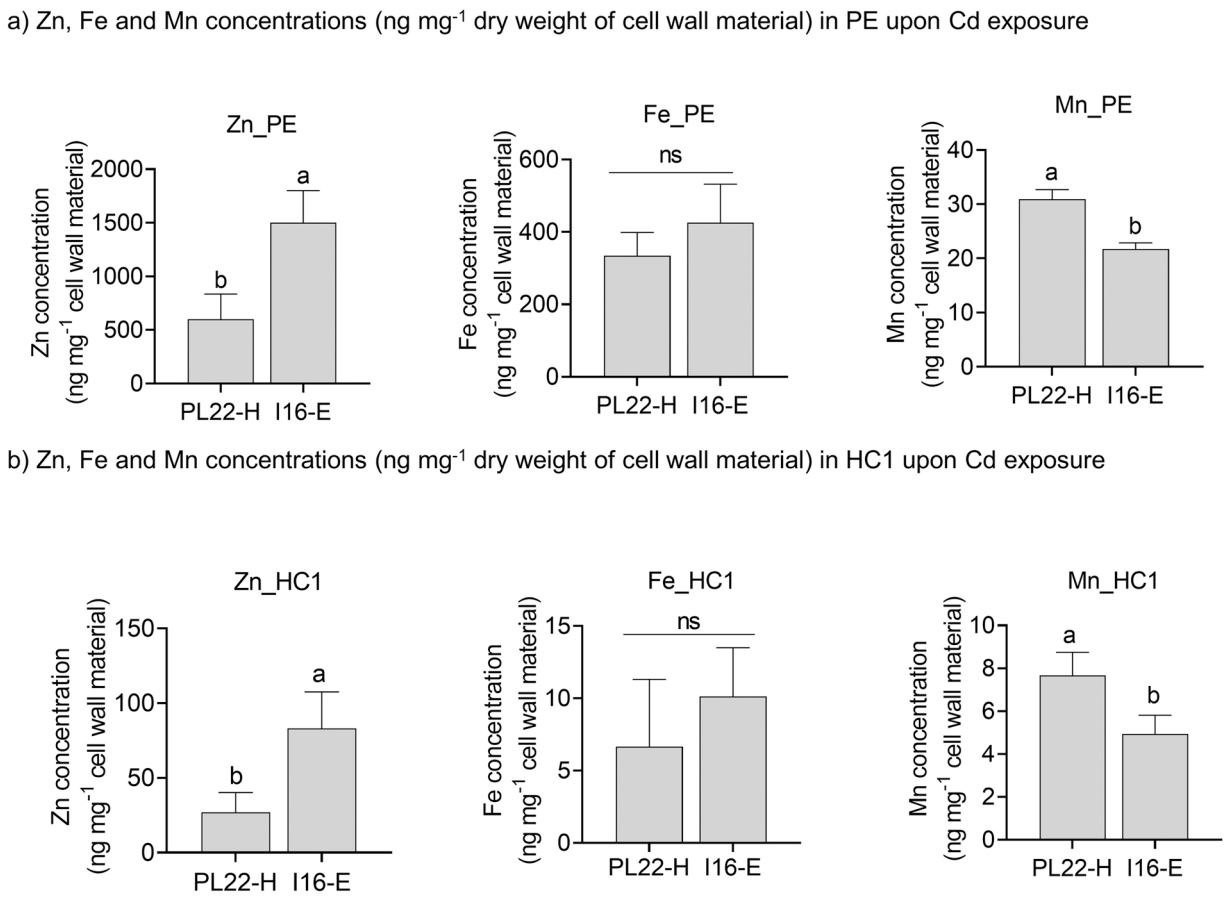

Fig. 7. Zn, Fe and Mn concentrations in pectin and hemicellulose of *A. halleri* roots. a, b) Zn, Fe, and Mn concentrations in PE (a) and HC1 (b) of PL22-H and I16-E plants grown in hydroponics upon Cd treatment. Different letters indicate statistically significant differences ($P < 0.05$) assessed by two-tailed t-test between PL22-H and I16-E. ns = not significant. Error bars represent the standard deviation (3 biological repetitions).

accordance with Kartel et al. (1999), who showed that metal binding properties of PEs were variable among different species and/or genotypes, e.g. beet PE exhibited strong affinities for Pb^{2+} and Cu^{2+}, while apple and citrus PEs showed high affinity for Co^{2+} and Ni^{2+}, respectively. These differences might be related to the charge density of PE, the ionic strength of the solution, and the strength of the interactions between the cation and PE (Renard and Jarvis, 1999; Krzesłowska, 2011).

In the current experiment, the HC content in I16-E was 1.7-fold higher than PL22-H upon Cd exposure (Fig. 1c). The HC contains carboxyl, hydroxyl, and aldehyde function groups, acting as metal sequestration sites (Park and Cosgrove, 2015). Previous studies showed that modification of CW composition (e.g. the changes of PE and HC contents and the degree of methyl-esterified PE) was responsible for the Cd fixation of the root (Zhu et al., 2013; Shi et al., 2015; Yu et al., 2018; Guo et al., 2020). Together the higher Cd binding capacity of the PE fraction and the higher HC content of I16-E compared to PL22-H could play a role in the higher Cd translocation factor of PL22-H. Finally, we showed that the ratio of HC2 to HC1 decreased in both PL22-H and I16-E upon Cd exposure (Fig. 1e), suggesting that Cd treatment induced CW modification at the level of polysaccharide interactions. HC1 and HC2 are gradually extracted by increasing alkali concentration, which induce the degradation of ester linkages and hydrogen bonds. (Renard and Ginies, 2009).

4.2. (1→4)-β-galactan may affect Cd translocation by regulating the length of RG-I sidechains, cell wall structure and polysaccharides interactions

From the glycan array analysis, (1→5)-α-arabinan and (1→4)-β-galactan of the PE fraction of roots showed the largest difference between PL22-H and I16-E, and were more abundant in I16-E. Accordingly, *ARAD2* and *GALS1* were also more expressed in I16-E than in PL22-H. Those polysaccharides are usually detected as sidechains of RG-I, a major PE component (Voragen et al., 2009). These sidechains play a crucial role in CW architecture and impact the rheological properties such as gelling, viscosity, solubility, porosity and elasticity elastic of PE (Hwang et al., 1993; Sousa et al., 2015).

Data presented in this study support a role for (1→4)-β-galactan in the regulation of Cd accumulation in *A. halleri* and *A. thaliana.* Although previous studies suggested that (1→4)-β-galactan was involved in cell elongation in etiolated hypocotyls and internodes (Moneo-Sánchez et al., 2019), regulation of CW water-binding capacity (Klaassen and Trindade, 2020), response to biotic and abiotic stress (Jaskowiak et al., 2019; Yan et al., 2021), and the maintenance of CW architecture (Carpita and Gibeaut, 1993; Cosgrove, 2005), the role of this pectic polysaccharide in TM accumulation remains poorly understood. On the contrary, we could not find evidence for a role of (1→5)-α-arabinan in Cd accumulation.

In the current study, *A. thaliana gals1–1 KO* mutant and the *GALS1* overexpressor showed a higher accumulation in the shoot and a higher root-to-shoot translocation of Cd, but also of Zn than the WT (Fig. 4d, f). A higher accumulation of Mn in the shoots of *gals1–1* was also detected as well as a higher Mn translocation in all *gals1* mutants and *OE-GALS1#5* (Fig. 4d, f). While *GALS1 KO* and *OE* mutants had different *GALS1* expression levels and galactose contents (Figs. S5b, 5a), they both showed an increase in the length of RG-I sidechains (galactan and arabinogalactan) after Cd treatment, in contrast to WT roots (Fig. 5b). This could partially explain the similar phenotypes observed in *glas1–1*

and *OE-GALS1#5* mutants. All together these results suggest that (1→4)-β-galactan does not directly bind Cd or acts as a Cd barrier, but might indirectly affect Cd (and Zn) accumulation by changing CW architecture and properties, such as porosity.

In *A. halleri*, the length of RG-I sidechains of the root CW was longer in PL22-H than in I16-E in the control condition, but it was the reverse after Cd treatment (Fig. 2b). It is difficult to account for the difference of results observed in *A. thaliana* and *A. halleri*. The length of the RG-I chains, and the composition of the CW in general are different in *A. thaliana* and *A. halleri*, and several factors other than the CW intervene to explain the differences in metal transport between these two species. The comparison between two contrasting populations of *A. halleri*, and the comparison of CWs allowed us to identify several differentially expressed CW-related genes possibly involved in Cd accumulation, but these genes cannot be expected to act independently of their cellular environment, which is very different between the two species studied.

We speculate that (1→4)-β-galactan may affect CW properties and Cd accumulation by jointly altering the length of RG-I sidechains, the PE structure (HG: RG-I) and interactions between polysaccharides, such as cellulose, xyloglucan.

First, *GALS1* is a bifunctional glycosyltransferase catalysing both extension and termination of pectic galactan oligosaccharides, which explains the link between *GALS1* and the length of RG-I galactan sidechain (Gal: Rha) (Laursen et al., 2018). Klaassen and Trindade (2020) hypothesized that the length of RG-I galactan sidechains together with CW remodeling (aggregation or loosening of CW) affected polysaccharides interactions in the matrix, CW structure and porosity. Second, the PE structure (low HG: RG-I) was modified by Cd treatment both in PL22-H and I16-E (Fig. 2b). Low HG: RG-I ratio was associated to a low degree of rigidity and intrinsic viscosity of the macromolecule (Kaya et al., 2014). Hence, HG: RG-I reduction in *OE-GALS1#5*, PL22-H and I16-E after Cd treatment (Figs. 2b, 5b) suggested that Cd induced a higher flexibility of modified PE in these plants, while we cannot precise the exact changes in CW structure as well as how it affects Cd accumulation. Third, (1→4)-β-galactan and xyloglucan signal intensities changed differently between PL22-H and I16-E after Cd treatment (Fig. 3b). Previous research reported that RG-I galactan sidechains could interact with xyloglucan and cellulose microfibrils (McCann and Roberts, 1991; Talbott and Ray, 1992; Carpita and Gibeaut, 1993). It has been demonstrated that (1→4)-β-galactan can influence the xyloglucan structure and the interaction between cellulose and xyloglucan, and is involved in CW reorganization (Moneo-Sánchez et al., 2019, 2020).

CW biosynthesis and properties are governed by multiple factors and several enzymes that work in a complex orchestrate its regulation. Although our results shed light about the role of (1→4)-β-galactan in metal accumulation and translocation, further investigation are needed to elucidate its function in the modulation of CW properties.

Besides the role of (1→4)-β-galactan in Cd accumulation described in this study, previous research showed that low-methylesterified HG can bind Cd (Krzesłowska, 2011; Guo et al., 2021). LM18 and LM19 mAbs used in this study, can partially recognize low-methyl-esterified HG, but can also bind to un-esterified HG. LM18 mAb recognises trigalacturonide epitopes, but LM19 mAb does not recognise oligogalacturonides with a degree of polymerization lower than four (Verhertbruggen et al., 2009). Nevertheless, LM18 and LM19 mAbs showed comparable signal intensities between PL22-H and I16-E (Fig. 3a), suggesting that the level of HG methylesterification does not contribute to contrasting Cd accumulation strategies between these *A. halleri* populations. However, several *A. halleri* CW-related DEGs were involved in PE methyl-esterification and their corresponding Arabidopsis mutants showed altered Cd accumulation. This should be investigated more in detail in the future.

4.3. Other cell wall-related genes affect Cd accumulation in Arabidopsis

Besides *arad2* and *gals1*, other *A. thaliana KO* mutants corresponding to *A. halleri* CW-related DEGs were screened for their involvement in Cd tolerance and accumulation (Fig. 6, Table 2).

The *bdx and luh KO* mutants, corresponding to genes more expressed in I16-E than in PL22-H, showed higher Cd accumulation compared to the WT, suggesting a role for *BDX* and *LUH* genes in the Cd exclusion strategy of I16-E. The *luh* mutant was also more tolerant to Cd (Fig. 6b; Table 2) than the WT (Fig. 6c, d; Table 2). Previous studies showed that the *luh* mutant was characterised by lower Al accumulation in roots and higher Al tolerance compared to the WT (Geng et al., 2017). LUH is a Groucho/TUP1 transcriptional co-repressor regulating PE modification (Liu and Karmarkar, 2008) but also PE methyl-esterification of HG as well as the RG-I structure (Western et al., 2001; Walker et al., 2011), which may account for its role in Cd accumulation in CW.

BDX encodes a BIIDXI, DUF642 CW protein, suggested to be involved in PE methyl esterase regulation (Zúñiga-Sánchez et al., 2014; Cruz-Valderrama et al., 2018). It is worth mentioning that the phenotype of *bdx* was stronger for Zn than for Cd, showing a 37% increase in Zn accumulation in shoots and a 19% increase in Zn translocation. This was also the case for *luh* with 51% more Zn in shoots and 45% higher Zn translocation compared to the WT. These results support a role for *BDX* and *LUH* in the lower Zn hyperaccumulation of I16-E compared to PL22-H observed by (Schvartzman et al., 2018).

5. Conclusion

This study explored the difference in CW monosaccharides, polysaccharides and the polymers of polysaccharides between Cd hyperaccumulating (PL22-H) and Cd excluding (I16-E) *A. halleri* populations. Cd tolerance and Cd accumulation of *A. thaliana* mutants corresponding to CW-related differentially expressed genes between those contrasting *A. halleri* plants were investigated.

These findings provide new insights into the role of CW components in Cd translocation and/or accumulation and can be further exploited to develop new strategies for phytoremediation or to limit the Cd accumulation in crops.

Environmental implication

Cadmium (Cd), a non-essential metal element toxic for animals and plants, is widespread in our environment. World Health Organization classified Cd as one of the top ten chemicals of major health concern based on scientific evidence and risk management. *Arabidopsis halleri* is a model for studying adaptation to extreme metallic environments. Our research investigated the role of cell wall components in Cd accumulation between Cd-accumulator and Cd-excluder *A. halleri* populations, which provided useful information for Cd phytoremediation and for understanding the mechanisms to limit Cd accumulation in crops.

Funding Sources

XA was financially supported by a doctoral grant from the Belgian Fund for Research training in Industry and Agriculture_FRIA (grants 5200220 F), a European Molecular Biology Organization (EMBO) Short-Term Fellowships (Nr. 8900) and a Van Buuren-Jaumotte-Demoulin Prize. The work was financially supported by the National Research Fund FNRS (PDR T.0120.18T.0120.18). This work has also benefited from the support of IJPB's Plant Observatory technological platforms. IJPB benefits from the support of Labex Saclay Plant Sciences-SPS (ANR-17-EUR-0007). The authors wish to thank the COST ACTION 19116 PLANTMETALS for efficient networking and discussion.

Credit authorship contribution statement

MC and NV designed and directed the research. XA, MC, CYJ, WW, AP, HH performed the glycan array experiment, analysed and/or interpret the data. JCT analysed the monosaccharides. MC and XA

Table 2
Cd tolerance and Cd accumulation capacity in *A. thaliana* mutants corresponding to cell wall-related differentially expressed genes in PL22-H and I16-E.

Gene name	Mutant	Expression in *A. halleri*	Cd tolerance test		Cd accumulation		Translocation factor
			Tissues				
			Root	Shoot	Root	Shoot	Shoot/root
PER39	*per39*	Higher expression in PL22	same	same	higher	higher	lower
PMEI18	*pmei18*		same	same	same	higher	same
APF2	*apf2*		same	same	same	–	–
CHITINASE	*chitinase*		lower	lower	same	–	–
LRX10	*lrx10*		same	same	same	–	–
LYSM	*lysm*	Higher expression in I16	lower	lower	same	–	–
BDX	*bdx*		lower	lower	higher	same	same
ARAD2	*arad2*		lower	lower	same	same	lower
WSCP	*wscp*		same	same	same	–	–
LUH	*luh*		higher	higher	higher	higher	same
GALS	*gals1–1*		higher	same	same	higher	higher
	gals1–2		same	same	same	same	same
	gals2		higher	same	same	higher	higher
	gals3		same	same	same	higher	same
	OE-GALS1#5		same	higher	same	higher	higher

Cd tolerance test was analyzed by measuring the primary root length, the lateral root length, and the number of lateral roots.
"higher", "same" and "lower" indicate measures compared with WT.
Shoot/Root: "higher" and "lower" indicate 10% higher or lower Cd translocation was in the mutants compared with the WT.
"—" = no data.

performed the ionomic analyses. XA measured CW polysaccharides and analysed physiological and ionome data. XA performed the analyses on *A. thaliana KO* mutants, generated all figures and supporting information. XA wrote the manuscript, which was extensively edited by NV and MC. All authors agree with the manuscript content.

Declaration of Competing Interest

The authors declare that they have no known competing financial interests or personal relationships that could have appeared to influence the work reported in this paper.

Data Availability

Data will be made available on request.

Acknowledgements

The authors would like to thank Michał Szopiński and Eugeniusz Małkowski (University of Silesia, Poland) for providing us the PL22-H seeds, and Roman Ceroni and Mauro Abbadini (Fattoria Ariete, Gorno, Italy) for providing I16-E seeds. We are also grateful to Sylvain Merlot and Sébastien Thomine (I2BC, CNRS, France) for their essential help with the measurement of metal content with MP-AES equipment.

Appendix A. Supporting information

Supplementary data associated with this article can be found in the online version at doi:10.1016/j.jhazmat.2022.130581.

References

Åkesson, A., Barregard, L., Bergdahl, I.A., Nordberg, G.F., Nordberg, M., Skerfving, S., 2014. Non-renal effects and the risk assessment of environmental cadmium exposure. Environ. Health Perspect. 122 (5), 431–438.
Arao, T., Takeda, H., Nishihara, E., 2008. Reduction of cadmium translocation from roots to shoots in eggplant (*Solanum melongena*) by grafting onto *Solanum torvum* rootstock. Soil Sci. Plant Nutr. 54 (4), 555–559.
Atmodjo, M.A., Hao, Z., Mohnen, D., 2013. Evolving views of pectin biosynthesis. Annu. Rev. Plant Biol. 64 (1), 747–779.
Bajpai P. 2018. Biermann's Handbook of Pulp and Paper: Volume 1: Raw Material and Pulp Making: Elsevier.
Baker, A.J., 1981. Accumulators and excluders-strategies in the response of plants to heavy metals. J. Plant Nutr. 3 (1–4), 643–654.
Baker, A.J., McGrath, S., Reeves, R.D., Smith, J., 2020. Metal hyperaccumulator plants: a review of the ecology and physiology of a biological resource for phytoremediation of metal-polluted soils. Phytoremediat. Contam. Soil Water 85–107.
Barberon, M., Vermeer, J.E., De Bellis, D., Wang, P., Naseer, S., Andersen, T.G., Humbel, B.M., Nawrath, C., Takano, J., Salt, D.E., et al., 2016. Adaptation of Root Function by Nutrient-Induced Plasticity of Endodermal Differentiation. Cell 164 (3), 447–459.
Blumenkrantz, N., Asboe-Hansen, G., 1973. New method for quantitative determination of uronic acids. Anal. Biochem. 54 (2), 484–489.
Broxterman, S.E., Schols, H.A., 2018. Interactions between pectin and cellulose in primary plant cell walls. Carbohydr. Polym. 192, 263–272.
Carpita, N.C., Gibeaut, D.M., 1993. Structural models of primary cell walls in flowering plants: consistency of molecular structure with the physical properties of the walls during growth. Plant J. 3 (1), 1–30.
Chaffei, C., 2003. Nitrogen metabolism of tomato under cadmium stress conditions. J. Plant Nutr. 26, 1617–1634.
Chen, X., Ouyang, Y., Fan, Y., Qiu, B., Zhang, G., Zeng, F., 2018. The pathway of transmembrane cadmium influx via calcium-permeable channels and its spatial characteristics along rice root. J. Exp. Bot. 69 (21), 5279–5291.
Clemens, S., 2006. Toxic metal accumulation, responses to exposure and mechanisms of tolerance in plants. Biochimie 88 (11), 1707–1719.
Clemens, S., 2019. Safer food through plant science: reducing toxic element accumulation in crops. J. Exp. Bot. 70 (20), 5537–5557.
Clemens, S., Ma, J.F., 2016. Toxic heavy metal and metalloid accumulation in crop plants and foods. Annu. Rev. Plant Biol. 67 (1), 489–512.
Clemens, S., Aarts, M.G., Thomine, S., Verbruggen, N., 2013. Plant science: the key to preventing slow cadmium poisoning. Trends Plant Sci. 18 (2), 92–99.
Corso, M., Schvartzman, M.S., Guzzo, F., Souard, F., Malkowski, E., Hanikenne, M., Verbruggen, N., 2018. Contrasting cadmium resistance strategies in two metallicolous populations of *Arabidopsis halleri*. N. Phytol. 218 (1), 283–297.
Corso, M., An, X., Jones, C.Y., Gonzalez-Doblas, V., Schvartzman, M.S., Malkowski, E., Willats, W.G., Hanikenne, M., Verbruggen, N., 2021. Adaptation of *Arabidopsis halleri* to extreme metal pollution through limited metal accumulation involves changes in cell wall composition and metal homeostasis. N. Phytol. 230 (2), 669–682.
Cosgrove, D.J., 2005. Growth of the plant cell wall. Nat. Rev. Mol. Cell Biol. 6 (11), 850–861.
Cruz-Valderrama, J.E., Jiménez-Durán, K., Zúñiga-Sánchez, E., Salazar-Iribe, A., Márquez-Guzmán, J., Gamboa-deBuen, A., 2018. Degree of pectin methyl esterification in endosperm cell walls is involved in embryo bending in *Arabidopsis thaliana*. Biochem Biophys. Res Commun. 495 (1), 639–645.
Dixon, R.A., Barros, J., 2019. Lignin biosynthesis: old roads revisited and new roads explored. Open Biol. 9 (12), 190215.
Dubois, M., Gilles, K.A., Hamilton, J.K., Rebers, Pt, Smith, F., 1956. Colorimetric method for determination of sugars and related substances. Anal. Chem. 28 (3), 350–356.
El Rasafi, T., Oukarroum, A., Haddioui, A., Song, H., Kwon, E.E., Bolan, N., Tack, F.M., Sebastian, A., Prasad, M., Rinklebe, J., 2022. Cadmium stress in plants: a critical review of the effects, mechanisms, and tolerance strategies. Crit. Rev. Environ. Sci. Technol. 52 (5), 675–726.
Ge, H., Huang, H., Xu, M., Chen, Q., 2016. Cellulose/poly (ethylene imine) composites as efficient and reusable adsorbents for heavy metal ions. Cellulose 23 (4), 2527–2537.
Genchi, G., Sinicropi, M.S., Lauria, G., Carocci, A., Catalano, A., 2020. The effects of cadmium toxicity. Int. J. Environ. Res. Public Health 17 (11), 3782.
Geng, X., Horst, W.J., Golz, J.F., Lee, J.E., Ding, Z., Yang, Z.B., 2017. *LEUNIG_HOMOLOG* transcriptional co-repressor mediates aluminium sensitivity through

PECTIN METHYLESTERASE 46-modulated root cell wall pectin methylesterification in Arabidopsis. Plant J. 90 (3), 491–504.
Gouia, H., Suzuki, A., Brulfert, J., Ghorbal, M.H., 2003. Effects of cadmium on the co-ordination of nitrogen and carbon metabolism in bean seedlings. J. Plant Physiol. 160 (4), 367–376.
Grant, C.A., Clarke, J.M., Duguid, S., Chaney, R., 2008. Selection and breeding of plant cultivars to minimize cadmium accumulation. Sci. Total Environ. 390 (2–3), 301–310.
Guimarães, Md.A., Gustin, J.L., Salt, D.E., 2009. Reciprocal grafting separates the roles of the root and shoot in zinc hyperaccumulation in *Thlaspi caerulescens*. N. Phytol. 184 (2), 323–329.
Guo, X., Liu, Y., Zhang, R., Luo, J., Song, Y., Li, J., Wu, K., Peng, L., Liu, Y., Du, Y., 2020. Hemicellulose modification promotes cadmium hyperaccumulation by decreasing its retention on roots in *Sedum alfredii*. Plant Soil 447 (1), 241–255.
Guo, X., Luo, J., Du, Y., Li, J., Liu, Y., Liang, Y., Li, T., 2021. Coordination between root cell wall thickening and pectin modification is involved in cadmium accumulation in *Sedum alfredii*. Environ. Pollut. 268, 115665.
Hanikenne, M., Nouet, C., 2011. Metal hyperaccumulation and hypertolerance: a model for plant evolutionary genomics. Curr. Opin. Plant Biol. 14 (3), 252–259.
Harholt, J., Jensen, J.K., Verhertbruggen, Y., Søgaard, C., Bernard, S., Nafisi, M., Poulsen, C.P., Geshi, N., Sakuragi, Y., Driouich, A., 2012. ARAD proteins associated with pectic Arabinan biosynthesis form complexes when transiently overexpressed in planta. Planta 236 (1), 115–128.
Harris, P.J., Stone, B.A., 2009. Chemistry and molecular organization of plant cell walls. Biomass. Recalcitrance: Deconstr. Plant Cell Wall Bioenergy 61–93.
Hu, J., Wu, F., Wu, S., Cao, Z., Lin, X., Wong, M.H., 2013. Bioaccessibility, dietary exposure and human risk assessment of heavy metals from market vegetables in Hong Kong revealed with an in vitro gastrointestinal model. Chemosphere 91 (4), 455–461.
Hwang, J., Pyun, Y., Kokini, J., 1993. Sidechains of pectins: some thoughts on their role in plant cell walls and foods. Food Hydrocoll. 7 (1), 39–53.
Jaskowiak, J., Kwasniewska, J., Milewska-Hendel, A., Kurczynska, E.U., Szurman-Zubrzycka, M., Szarejko, I., 2019. Aluminum alters the histology and pectin cell wall composition of barley roots. Int. J. Mol. Sci. 20 (12), 3039.
Kaczmarska, A., Pieczywek, P.M., Cybulska, J., Zdunek, A., 2021. Structure and functionality of Rhamnogalacturonan I in the cell wall and in solution: a review. Carbohydr. Polym., 118909
Kartel, M.T., Kupchik, L.A., Veisov, B.K., 1999. Evaluation of pectin binding of heavy metal ions in aqueous solutions. Chemosphere 38 (11), 2591–2596.
Kaya, M., Sousa, A.G., Crépeau, M.-J., Sørensen, S.O., Ralet, M.-C., 2014. Characterization of citrus pectin samples extracted under different conditions: influence of acid type and pH of extraction. Ann. Bot. 114 (6), 1319–1326.
Klaassen, M.T., Trindade, L.M., 2020. RG-I galactan side-chains are involved in the regulation of the water-binding capacity of potato cell walls. Carbohydr. Polym. 227, 115353.
Kopittke, P.M., Blamey, F.P.C., Asher, C.J., Menzies, N.W., 2010. Trace metal phytotoxicity in solution culture: a review. J. Exp. Bot. 61 (4), 945–954.
Koren'kov, V., Park, S., Cheng, N.-H., Sreevidya, C., Lachmansingh, J., Morris, J., Hirschi, K., Wagner, G., 2007. Enhanced Cd2+-selective root-tonoplast-transport in tobaccos expressing Arabidopsis cation exchangers. Planta 225 (2), 403–411.
Krämer, U., 2010. Metal hyperaccumulation in plants. Annu. Rev. Plant Biol. 61 (1), 517–534.
Krzesłowska, M., 2011. The cell wall in plant cell response to trace metals: polysaccharide remodeling and its role in defense strategy. Acta Physiol. Plant. 33 (1), 35–51.
Laursen, T., Stonebloom, S.H., Pidatala, V.R., Birdseye, D.S., Clausen, M.H., Mortimer, J. C., Scheller, H.V., 2018. Bifunctional glycosyltransferases catalyze both extension and termination of pectic galactan oligosaccharides. Plant J. 94 (2), 340–351.
Liu, Z., Karmarkar, V., 2008. Groucho/Tup1 family co-repressors in plant development. Trends Plant Sci. 13 (3), 137–144.
Liwanag, A.J.M., Ebert, B., Verhertbruggen, Y., Rennie, E.A., Rautengarten, C., Oikawa, A., Andersen, M.C., Clausen, M.H., Scheller, H.V., 2012. Pectin biosynthesis: *GALS1* in *Arabidopsis thaliana* is a β-1, 4-galactan β-1, 4-galactosyltransferase. Plant Cell 24 (12), 5024–5036.
Loix, C., Huybrechts, M., Vangronsveld, J., Gielen, M., Keunen, E., Cuypers, A., 2017. Reciprocal interactions between cadmium-induced cell wall responses and oxidative stress in plants. Front. Plant Sci. 8, 1867.
McCann, M., Roberts, K., 1991. The cytoskeletal basis of plant growth and form. Lloyd, C. W. ed. London, Academic Press.
Meyer, C.-L., Juraniec, M., Huguet, S., Chaves-Rodriguez, E., Salis, P., Isaure, M.-P., Goormaghtigh, E., Verbruggen, N., 2015. Intraspecific variability of cadmium tolerance and accumulation, and cadmium-induced cell wall modifications in the metal hyperaccumulator *Arabidopsis halleri*. J. Exp. Bot. 66 (11), 3215–3227.
Moller, I., Sorensen, I., Bernal, A.J., Blaukopf, C., Lee, K., Obro, J., Pettolino, F., Roberts, A., Mikkelsen, J.D., Knox, J.P., et al., 2007. High-throughput mapping of cell-wall polymers within and between plants using novel microarrays. Plant J. 50 (6), 1118–1128.
Moller, I.E., Pettolino, F.A., Hart, C., Lampugnani, E.R., Willats, W.G., Bacic, A., 2012. Glycan profiling of plant cell wall polymers using microarrays. J. Vis. Exp. 70, e4238.
Moneo-Sánchez, M., Alonso-Chico, A., Knox, J.P., Dopico, B., Labrador, E., Martín, I., 2019. β-(1, 4)-Galactan remodelling in Arabidopsis cell walls affects the xyloglucan structure during elongation. Planta 249 (2), 351–362.
Moneo-Sánchez, M., Vaquero-Rodríguez, A., Hernández-Nistal, J., Albornos, L., Knox, P., Dopico, B., Labrador, E., Martín, I., 2020. Pectic galactan affects cell wall architecture during secondary cell wall deposition. Planta 251 (5), 1–15.
O'Connell, D., Birkinshaw, C., O'dwyer, T., 2008. Removal of copper, nickel and lead from wastewater using a modified cellulose material: a comparison. WIT Trans. Ecol. Environ. 109, 809–818.
Papoyan, A., Kochian, L.V., 2004. Identification of Thlaspi caerulescens genes that may be involved in heavy metal hyperaccumulation and tolerance. Characterization of a novel heavy metal transporting ATPase. Plant Physiol. 136 (3), 3814–3823.
Park, Y.B., Cosgrove, D.J., 2015. Xyloglucan and its interactions with other components of the growing cell wall. Plant Cell Physiol. 56 (2), 180–194.
Parrotta, L., Guerriero, G., Sergeant, K., Cai, G., Hausman, J.-F., 2015. Target or barrier? The cell wall of early-and later-diverging plants vs cadmium toxicity: differences in the response mechanisms. Front. Plant Sci. 6, 133.
Pauwels, M., Vekemans, X., Godé, C., Frérot, H., Castric, V., Saumitou-Laprade, P., 2012. Nuclear and chloroplast DNA phylogeography reveals vicariance among European populations of the model species for the study of metal tolerance, *Arabidopsis halleri* (Brassicaceae). N. Phytol. 193 (4), 916–928.
Pittman, J.K., Shigaki, T., Marshall, J.L., Morris, J.L., Cheng, N.-H., Hirschi, K.D., 2004. Functional and regulatory analysis of the Arabidopsis thaliana CAX2 cation transporter. Plant Mol. Biol. 56 (6), 959–971.
Pound, M.P., French, A.P., Atkinson, J.A., Wells, D.M., Bennett, M.J., Pridmore, T., 2013. RootNav: navigating images of complex root architectures. Plant Physiol. 162 (4), 1802–1814.
Renard, C., Jarvis, M., 1999. Acetylation and methylation of homogalacturonans 2: effect on ion-binding properties and conformations. Carbohydr. Polym. 39 (3), 209–216.
Renard, C.M., Ginies, C., 2009. Comparison of the cell wall composition for flesh and skin from five different plums. Food Chem. 114 (3), 1042–1049.
Renard, C.M., Lahaye, M., Mutter, M., Voragen, F.G., Thibault, J.-F., 1997. Isolation and structural characterisation of rhamnogalacturonan oligomers generated by controlled acid hydrolysis of sugar-beet pulp. Carbohydr. Res. 305 (2), 271–280.
Rose, J.K., 2003. The Plant Cell Wall. In: Rose, J.K. (Ed.). Oxford, CRC Press.
San Clemente, H., Jamet, E., 2015. WallProtDB, a database resource for plant cell wall proteomics. Plant Methods 11 (1), 1–7.
Schindelin, J., Arganda-Carreras, I., Frise, E., Kaynig, V., Longair, M., Pietzsch, T., Preibisch, S., Rueden, C., Saalfeld, S., Schmid, B., 2012. Fiji: an open-source platform for biological-image analysis. Nat. Methods 9 (7), 676–682.
Schutzendubel, A., Polle, A., 2002. Plant responses to abiotic stresses: heavy metal-induced oxidative stress and protection by mycorrhization. J. Exp. Bot. 53 (372), 1351–1365.
Schvartzman, M.S., Corso, M., Fataftah, N., Scheepers, M., Nouet, C., Bosman, B., Carnol, M., Motte, P., Verbruggen, N., Hanikenne, M., 2018. Adaptation to high zinc depends on distinct mechanisms in metallicolous populations of *Arabidopsis halleri*. N. Phytol. 218 (1), 269–282.
Shi, Y.Z., Zhu, X.F., Wan, J.X., Li, G.X., Zheng, S.J., 2015. Glucose alleviates cadmium toxicity by increasing cadmium fixation in root cell wall and sequestration into vacuole in Arabidopsis. J. Integr. Plant Biol. 57 (10), 830–837.
Siedlecka, A., BaszyńAski, T., 1993. Inhibition of electron flow around photosystem I in chloroplasts of Cd-treated maize plants is due to Cd-induced iron deficiency. Physiol. Plant. 87 (2), 199–202.
Sousa, A.G., Nielsen, H.L., Armagan, I., Larsen, J., Sørensen, S.O., 2015. The impact of rhamnogalacturonan-I side chain monosaccharides on the rheological properties of citrus pectin. Food Hydrocoll. 47, 130–139.
Suhani, I., Sahab, S., Srivastava, V., Singh, R.P., 2021. Impact of cadmium pollution on food safety and human health. Curr. Opin. Toxicol. 27, 1–7.
Talbott, L.D., Ray, P.M., 1992. Changes in molecular size of previously deposited and newly synthesized pea cell wall matrix polysaccharides: effects of auxin and turgor. Plant Physiol. 98 (1), 369–379.
Tian, T., Liu, Y., Yan, H., You, Q., Yi, X., Du, Z., Xu, W., Su, Z., 2017. agriGO v2. 0: a GO analysis toolkit for the agricultural community, 2017 update. Nucleic Acids Res. 45 (W1), W122–W129.
Ursache, R., Andersen, T.G., Marhavy, P., Geldner, N., 2018. A protocol for combining fluorescent proteins with histological stains for diverse cell wall components. Plant J. 93 (2), 399–412.
Verbruggen, N., Hermans, C., Schat, H., 2009a. Mechanisms to cope with arsenic or cadmium excess in plants. Curr. Opin. Plant Biol. 12 (3), 364–372.
Verbruggen, N., Hermans, C., Schat, H., 2009b. Molecular mechanisms of metal hyperaccumulation in plants. N. Phytol. 181 (4), 759–776.
Verbruggen, N., Juraniec, M., Baliardini, C., Meyer, C.-L., 2013. Tolerance to cadmium in plants: the special case of hyperaccumulators. Biometals 26 (4), 633–638.
Voragen, A.G., Coenen, G.-J., Verhoef, R.P., Schols, H.A., 2009. Pectin, a versatile polysaccharide present in plant cell walls. Struct. Chem. 20 (2), 263–275.
Wagner, G.J., 1988. Root control of leaf cadmium accumulation in tobacco. Tob. Sci. 32, 88–91.
Walker, M., Tehseen, M., Doblin, M.S., Pettolino, F.A., Wilson, S.M., Bacic, A., Golz, J.F., 2011. The transcriptional regulator LEUNIG_HOMOLOG regulates mucilage release from the Arabidopsis testa. Plant Physiol. 156 (1), 46–60.
Wang, L., Li, R., Yan, X., Liang, X., Sun, Y., Xu, Y., 2020. Pivotal role for root cell wall polysaccharides in cultivar-dependent cadmium accumulation in *Brassica chinensis L.* Ecotoxicol. Environ. Saf. 194, 110369.
Wang, P., Yang, B., Wan, H., Fang, X., Yang, C., 2018. The differences of cell wall in roots between two contrasting soybean cultivars exposed to cadmium at young seedlings. Environ. Sci. Pollut. Res. 25 (29), 29705–29714.
Wei, L., Luo, C., Li, X., Shen, Z., 2008. Copper accumulation and tolerance in *Chrysanthemum coronarium L.* and *Sorghum sudanense L.* Arch. Environ. Contam. Toxicol. 55 (2), 238–246.
Western, T.L., Burn, J., Tan, W.L., Skinner, D.J., Martin-McCaffrey, L., Moffatt, B.A., Haughn, G.W., 2001. Isolation and characterization of mutants defective in seed coat

mucilage secretory cell development in Arabidopsis. Plant Physiol. 127 (3), 998–1011.
Xiao, Y., Dai, M.-X., Zhang, G.-Q., Yang, Z.-X., He, Y.-M., Zhan, F.-D., 2021. Effects of the Dark Septate Endophyte (DSE) *Exophiala pisciphila* on the Growth of Root Cell Wall Polysaccharides and the Cadmium Content of *Zea mays L.* under Cadmium Stress. J. Fungi 7 (12), 1035.
Yan, J., Liu, Y., Yang, L., He, H., Huang, Y., Fang, L., Scheller, H.V., Jiang, M., Zhang, A., 2021. Cell wall β-1, 4-galactan regulated by the BPC1/BPC2-GALS1 module aggravates salt sensitivity in *Arabidopsis thaliana*. Mol. Plant 14 (3), 411–425.
Yang, J.L., Li, Y.Y., Zhang, Y.J., Zhang, S.S., Wu, Y.R., Wu, P., Zheng, S.J., 2008. Cell wall polysaccharides are specifically involved in the exclusion of aluminum from the rice root apex. Plant Physiol. 146 (2), 602–611.
Yi, L., Shi, S., Yi, Z., He, R., Lu, H., Liang, Y., 2014. MeOx-TMS derivatization for GC-MS metabolic profiling of urine and application in the discrimination between normal C57BL/6J and type 2 diabetic KK-Ay mice. Anal. Methods 6 (12), 4380–4387.
Yu, H., Wu, Y., Huang, H., Zhan, J., Wang, K., Li, T., 2020. The predominant role of pectin in binding Cd in the root cell wall of a high Cd accumulating rice line (*Oryza sativa L.*). Ecotoxicol. Environ. Saf. 206, 111210.
Yu, Y., Zhou, X., Zhu, Z., Zhou, K., 2018. Sodium hydrosulfide mitigates cadmium toxicity by promoting cadmium retention and inhibiting its translocation from roots to shoots in *Brassica napus*. J. Agric. Food Chem. 67 (1), 433–440.
Zhong, H., Lauchli, A., 1993. Changes of cell wall composition and polymer size in primary roots of cotton seedlings under high salinity. J. Exp. Bot. 44 (4), 773–778.
Zhu, X.F., Wang, Z.W., Dong, F., Lei, G.J., Shi, Y.Z., Li, G.X., Zheng, S.J., 2013. Exogenous auxin alleviates cadmium toxicity in *Arabidopsis thaliana* by stimulating synthesis of hemicellulose 1 and increasing the cadmium fixation capacity of root cell walls. J. Hazard Mater. 263, 398–403.
Zúñiga-Sánchez, E., Soriano, D., Martínez-Barajas, E., Orozco-Segovia, A., Gamboa-deBuen, A., 2014. *BIIDXI*, the *At4g32460* DUF642 gene, is involved in pectin methyl esterase regulation during *Arabidopsis thaliana* seed germination and plant development. BMC Plant Biol. 14 (1), 1–13.